

Crystal Plasticity Finite-Element Simulations of Cup Drawing of a ZX10 Magnesium Alloy Sheet

Takayuki Hama^{1,a*} and Naoki Miyazawa^{1,b}

¹Graduate School of Energy Science, Kyoto University, Yoshida-Honmachi, Sakyo-ku, Kyoto, 606-8501, Japan

^{a*}hama@energy.kyoto-u.ac.jp, ^bmiyazawa.naoki.3n@kyoto-u.ac.jp

Keywords: magnesium alloy, cup drawing, twinning, crystal plasticity finite-element method.

Abstract. Magnesium (Mg) alloy sheets are expected to contribute to the lightweighting of structural components, owing to their inherent benefits of low density and high specific strength. However, the limited room-temperature press formability exhibited in Mg alloy sheets remains a barrier to their expanded use. A significant factor contributing to the limited formability is the strong basal texture. To improve the room-temperature press formability, ZX series Mg alloy sheets that weakened the basal texture have recently been developed. In our previous study [Hama et al., *Mater. Res. Proc.*, 28(2003), 711-716], cup drawability of a Mg-1.5mass%Zn-0.1mass%Ca (ZX10Mg) alloy sheet was investigated at room temperature. The obtained cup exhibited that the cup height and thickness strains differed significantly in the circumferential direction of the cup. However, a more detailed discussion on the mechanisms of this anisotropic deformation was hampered by a reliance solely on experimental observations. Therefore, in this study, crystal plasticity finite-element simulations of cup drawing of the ZX10Mg alloy sheet were performed. The simulation results qualitatively reproduced macroscopic and microscopic deformation behaviors during cup drawing. Numerical studies showed that the anisotropic deformation during drawing was primarily induced by the texture of the material, suggesting that anisotropic deformation is inevitable unless the anisotropic *c*-axes distribution remains in the initial texture.

Introduction

Magnesium (Mg) alloy sheets are expected to contribute to the lightweighting of structural components, owing to their inherent benefits of low density and high specific strength. However, the limited room-temperature press formability exhibited in Mg alloy sheets remains a barrier to their expanded use. A significant factor contributing to the limited formability is the strong basal texture, which is typically found in AZ-series rolled Mg alloy sheets. Therefore, Mg-Zn-Ca alloy sheets have been developed to improve the room-temperature press formability, which weakened the basal texture [1, 2]. Rolled Mg-1.5mass%Zn-0.1mass%Ca (ZX10Mg) alloy sheets were used to examine the room-temperature formability, including the work-hardening behavior [3, 4] and drawability [5]. Hama et al. [3] showed that the work-hardening behavior exhibited pronounced in-plane anisotropy and tension-compression asymmetry. Hama et al. [5] also reported that circular cup drawing could be achieved using this sheet, but the cup height and thickness strains differed significantly in the circumferential direction of the cup. Especially, the cup heights were notably different between the rolling direction (RD) and transverse direction (TD). Because the plastic deformation behavior of Mg alloy sheets is typically governed by both slip and twinning activities, this characteristic cup shape would result from a complicated combination of these activities. However, further discussions on the deformation mechanisms based solely on experimental observations was difficult.

In the present study, crystal plasticity finite-element simulations of circular cup drawing of a rolled ZX10Mg alloy sheet were performed at room temperature. The simulation results were first compared with the experimental results to verify the results. Thereafter, the drawability was discussed in detail based on the simulation results.

Material

Figure 1 (a) shows the (0001) pole figure of the ZX10Mg alloy sheet modeled in this study. This material was the same as that used in the previous study [3, 5]. The strong peaks that tilted from the ND to the TD appeared. Moreover, the c -axes orientations of the grains were notably spread in the TD, and the peaks near the TD also appeared. The distribution of the c -axes orientations was apparently anisotropic in the RD-TD plane.

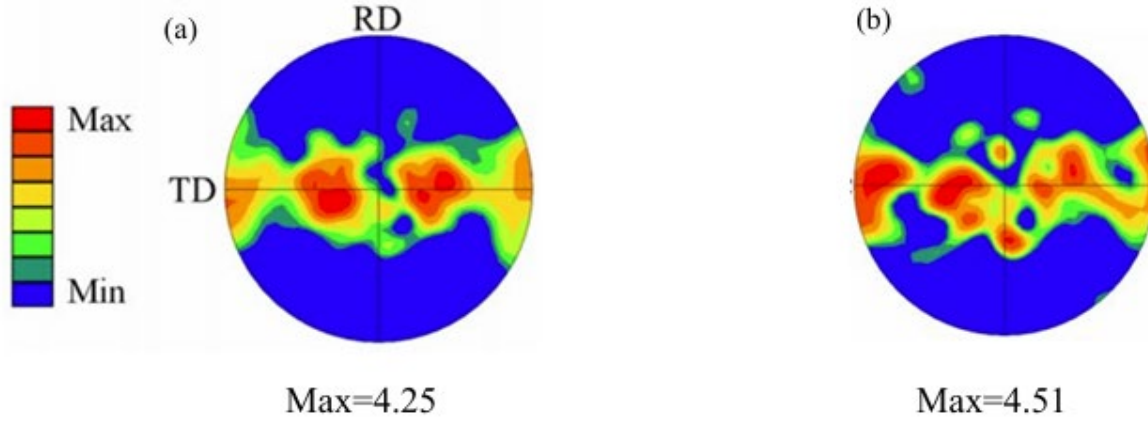


Fig. 1. (0001) pole figures of ZX10Mg alloy sheet used in this study. (a) Experiment and (b) simulation.

Crystal plasticity finite-element method

A crystal plasticity finite-element method used in this study is the same as those used in our previous studies [6-10]. Therefore, the model is explained only briefly. Assuming that the crystalline slip follows the Schmid's law, the slip rate $\dot{\gamma}^{(\alpha)}$ of the α slip system is given by the following equation.

$$\frac{\dot{\gamma}^{(\alpha)}}{\dot{\gamma}_0} = \left| \frac{\tau^{(\alpha)}}{\tau_Y^{(\alpha)}} \right|^{\frac{1}{m}} \text{sign}(\tau^{(\alpha)}), \quad \dot{\tau}_Y^{(\alpha)} = \sum_{\beta} q_{\alpha\beta} h \left| \dot{\gamma}^{(\beta)} \right|, \quad (1)$$

where $\tau^{(\alpha)}$ and $\tau_Y^{(\alpha)}$ are the Schmid's resolved shear stress and the slip resistance of the α slip system, respectively. $\dot{\gamma}_0$ is the reference strain rate, m is the rate sensitivity exponent, and $q_{\alpha\beta}$ represents the self- and latent- hardening moduli matrix. h is the rate of hardening and is given by the following equations.

$$h = h_0 \quad (2)$$

and

$$h = h_0 \left(1 - \frac{\tau_0}{\tau_\infty} \right) \exp \left(- \frac{h_0 \bar{\gamma}}{\tau_\infty} \right), \quad \bar{\gamma} = \sum_{\alpha} \int \left| \dot{\gamma}^{(\alpha)} \right| dt. \quad (3)$$

In this study, the basal slip $\langle a \rangle$, prismatic slip $\langle a \rangle$, pyramidal-2 slip $\langle a+c \rangle$, and $\{10\bar{1}2\}$ twinning were considered as the active slip and twinning systems in the ZX10 Mg alloy sheet. The linear hardening (Eq. (2)) was assumed for the basal slip and $\{10\bar{1}2\}$ twinning, whereas the Voce hardening (Eq. (3)) was assumed for the prismatic and pyramidal-2 slip. A twinning and detwinning model proposed by Hama et al. [7, 11] was employed. The crystal plasticity model was used as constitutive equations in the static finite-element method. The reader is referred to the literature [6-11] for more details.

The simulation conditions were determined based on the experiments reported in the literature [5]. Figure 2 shows the finite-element model of the circular sheet [12]. The thickness and diameter of the

sheet were respectively 1.0 mm and 40.0 mm. Assuming the symmetry of the deformation process, only the quarter part of the sheet was modeled using 1976 solid elements. The initial crystal orientations were determined based on the result of EBSD measurement, and 800 orientations were assigned to each integration point considering the Taylor assumption. Figure 1 (b) shows the (0001) pole figure obtained using the 800 orientations considered in the simulation. The experimental result is reproduced qualitatively well. The tools were assumed rigid. The diameters of die cavity and punch were respectively 30.0 mm and 27.8 mm. The radii of die and punch shoulders were respectively 7.0 mm and 5.0 mm. The gap between the die and blank holder was fixed to 1.1 mm. The friction coefficient was set to 0.03 to reasonably reproduce the punch load-stroke curve.

The hardening parameters in eqs. (2) and (3) were determined to fit the stress-strain curves under uniaxial tension and compression in the RD and TD. The stress-strain curves and determined parameters are shown in Figure 3 and Table 1, respectively. The stress-strain curves are well reproduced in the simulations, although the work-hardening behavior under tension were slightly deviated from the experimental results [3]. The fitting accuracy could be improved by further adjusting the parameters, but it is currently challenging from the following reason. In crystal plasticity simulations of Mg alloys, many parameters should be calibrated as shown in Table 1 because the slip activity differs significantly depending on the slip system. In our previous study on AZ-series Mg alloy sheets [10], we proposed a systematic procedure to calibrate the parameters separately for each slip system. This procedure worked well for AZ-series Mg alloy sheets because these sheets had strong basal textures; thus, the slip and twinning activities could be estimated rather systematically depending on the loading condition. By contrast, this procedure was not applicable for the present ZX10Mg alloy sheet because of the less-pronounced basal texture.

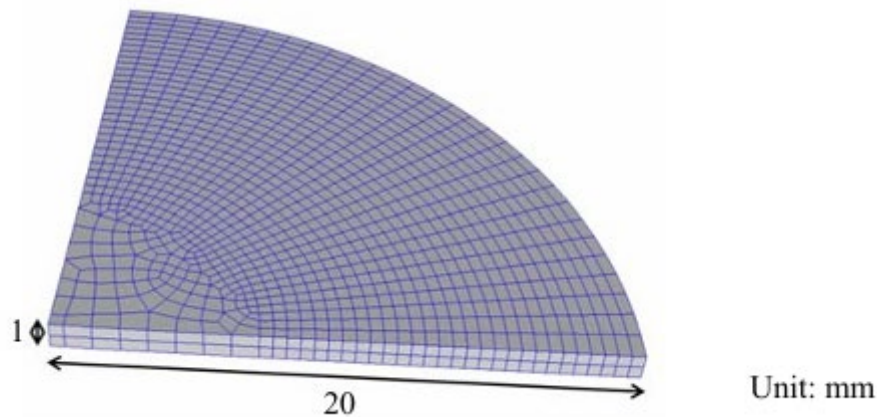


Fig. 2. Finite-element model used for cup drawing simulations.

Therefore, to improve the fitting accuracy, alternative procedures of parameter calibration should be established. This will be conducted in our future work.

Results and Discussion

Figure 4 shows the punch load-stroke curves obtained in the experiment and simulation. In the simulation, the maximum load at a punch stroke of approximately 9 mm was overestimated, whereas the local minimum value at a punch stroke of approximately 13 mm was well reproduced. The quantitative discrepancy between the experimental and simulation results might be due to several factors, including the friction coefficient, contact algorithm, and predictive accuracy of work-hardening behavior under multiaxial stress states.

Figure 5 (a) shows the cup height distribution in the circumferential direction obtained from the experimental [5] and simulation results of the drawn cup. Notably, the vertical axis represents the relative height in which the height in the RD was set to zero. The absolute height was not used because the cup bottom was rounded; thus, precise measurements were difficult. As explained in the literature [5], the experimental result showed the following trend. The height increased from the RD to the

angle of 60° , and then decreased gradually to the TD. The maximum height appeared at 60° . The height in the TD was larger than that in the RD. The simulation result well reproduced the distribution trend, although the maximum height was slightly underestimated.

Figure 5 (b) shows the thickness strain evolution at the cup edge in the RD and TD as a function of the punch stroke. In the experimental results [5], the thickness strains increased with the punch stroke until the punch stroke of 13 mm. In this stage, the thickness strains were the largest in the RD and the smallest in the TD. Thereafter, the thickness strains decreased sharply until the end of the process. This decrease occurred due to the ironing between the punch and die. The simulation results captured well these trends, although the strains in the angle of 45° (DD) and TD were respectively underestimated and overestimated.

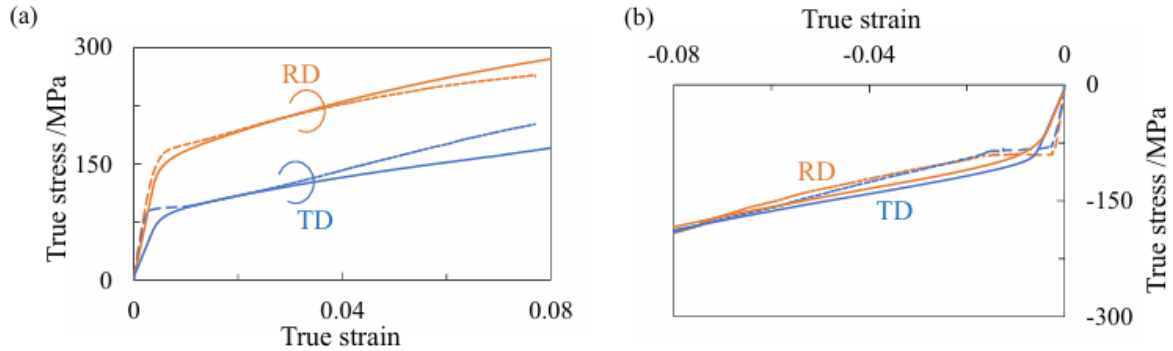


Fig. 3. True stress-true strain curves under (a) tension and (b) compression. The broken and solid lines are the experimental and simulation results, respectively.

Table 1. Material parameters for crystal-plasticity model.

	τ_0	τ_∞	h_0
<i>Basal</i>	3		10
<i>Prismatic</i>	80	350	1200
<i>Pyramidal</i>	80	200	1400
<i>Twinning</i>	3		5
<i>Detwinning</i>	3		5

Figure 6 shows the (0001) pole figures measured at the cup edges in the RD and TD. In the experimental results, pronounced texture evolution occurred because of twinning activities. Specifically, the strong peaks appeared near the TD at the RD edge, whereas they appeared near the RD at the TD edge. These trends were well reproduced in the simulation results. These texture evolutions at the RD and TD edges agree well with those observed under uniaxial compression in the TD and RD [3], respectively. These observations suggest that circumferential compression was dominant during drawing at the sheet edge rather than bending and unbending in the radial direction.

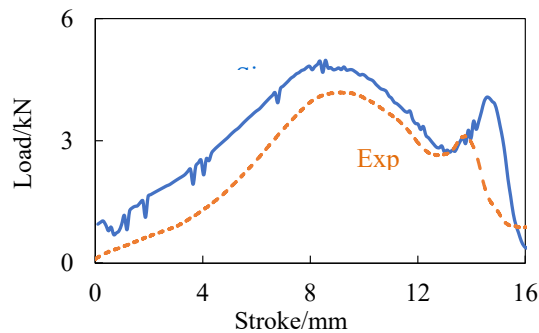


Fig. 4. Punch load-stroke curves obtained from experiment and simulation.

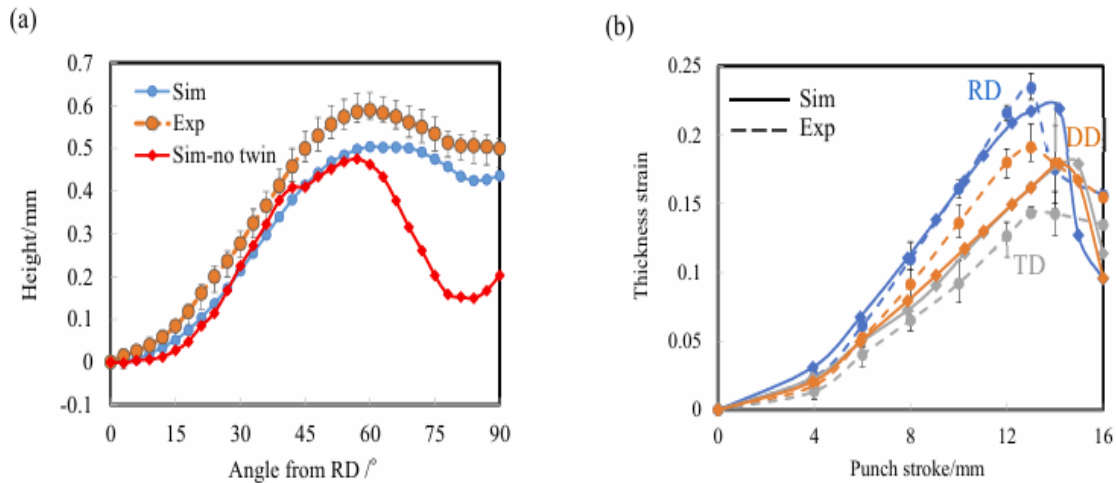


Fig. 5. Comparisons of deformation shapes between experiment and simulation. (a) Cup height distributions in circumferential direction and (b) thickness strain evolution at cup edges.

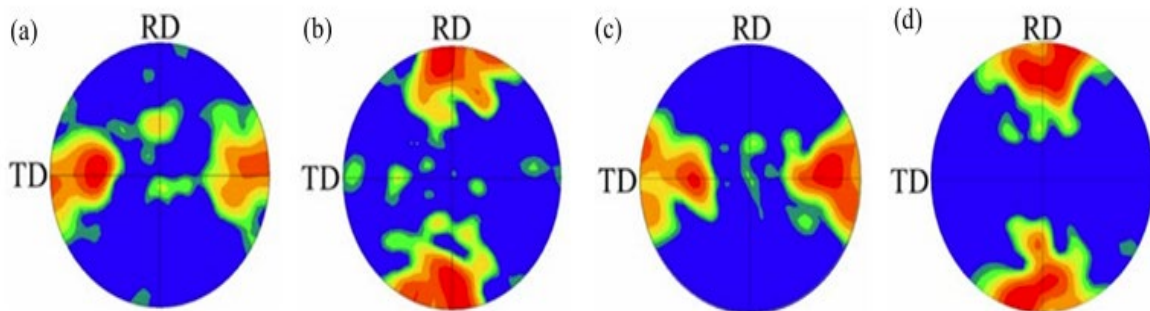


Fig. 6. (0001) pole figures measured on the drawn cup. Experimental results at the (a) RD edge and (b) TD edge, and simulation results at the (c) RD edge and (d) TD edge.

Hama et al. [13] studied the relationship between the Lankford value and twinning activity in the ZX10Mg alloy sheet and concluded that thickness strains induced by twinning activities affect the Lankford values both under RD and TD compression. This further suggests that the twinning activity during cup drawing should affect significantly the shape of drawn cup. To verify this hypothesis, a simulation was conducted without considering twinning activity. The simulation result without considering twinning is shown in Figure 5 (a). The cup height in the TD decreased and became close to that in the RD. These results show that twinning activities significantly affect the difference in the cup height between the RD and TD. Figure 7 shows the thickness strain evolution obtained from the simulation without considering twinning. The thickness strains to a stroke of 13 mm became smaller regardless of the direction when twinning was not considered, suggesting that the thickness increase during this process is affected notably by twinning activity. By contrast, the sharp decrease beyond a stroke of 13 mm became less pronounced, indicating that twinning activity also helped sharp decrease due to the ironing process. Notably, the anisotropic thickness strain evolution remained even when twinning was not considered. Because the twinning activity is governed by the texture, these results further suggest that anisotropic height distribution in the drawn cup might be inevitable unless the anisotropic c -axes distribution remains in the initial texture.

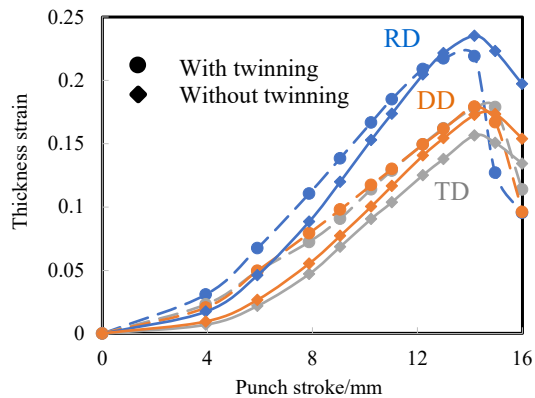


Fig. 7. Effect of twinning on thickness strain evolution at cup edges.

Conclusion

In this study, crystal plasticity finite-element simulations of circular cup drawing of a rolled ZX10Mg alloy sheet were performed at room temperature. The drawability of the material was discussed in detail based on the simulation results. The conclusions obtained in this study are summarized as follows.

- (1) Crystal plasticity simulations qualitatively reproduced macroscopic and microscopic deformation behaviors during cup drawing of the ZX10 Mg alloy sheet.
- (2) Simulation results showed that twinning activities affected notably the shape of drawn cup.
- (3) Anisotropic deformation during drawing was induced by the texture, suggesting that anisotropic deformation is inevitable unless the anisotropic *c*-axes distribution remains in the initial texture.

References

- [1] Y. Chino, X. Huang, K. Suzuki, M. Mabuchi, Enhancement of stretch formability at room temperature by addition of Ca in Mg-Zn alloy, *Mater. Trans.*, 51 (2010), 818–821, <https://doi.org/10.2320/matertrans.M2009385>.
- [2] Y. Chino, T. Ueda, Y. Otomatsu, K. Sassa, X. Huang, K. Suzuki, M. Mabuchi, Effects of Ca on tensile properties and stretch formability at room temperature in Mg-Zn and Mg-Al alloys, *Mater. Trans.*, 52 (2011), 1477–1482. <https://doi.org/10.2320/matertrans.M2011048>.
- [3] T. Hama, T. Nakata, K. Higuchi, H. Yoshida, Y. Jono, Plastic deformation behavior of a Mg-1.5Zn-0.1Ca (mass%) alloy sheet under different strain paths, *Mater. Sci. Eng. A*, 869(2023), 144772. <https://doi.org/10.1016/j.msea.2023.144772>.
- [4] T. Nakata, T. Hama, K. Sugaya, S. Kamado, Understanding room-temperature deformation behavior in a dilute Mg-1.52Zn-0.09Ca(mass%) alloy sheet with weak basal texture, *Mater. Sci. Eng. A*, 852 (2022), 143638. <https://doi.org/10.1016/j.msea.2022.143638>.
- [5] T. Hama, K. Higuchi, Y. Nakata, Anisotropic deformation behavior during cup drawing at room temperature of a ZX10 magnesium alloy sheet, *Mater. Res. Proc.*, 28(2023), 711-716.
- [6] T. Hama, H. Takuda, Crystal-plasticity finite-element analysis of inelastic behavior during unloading in a Magnesium alloy sheet, *Int J Plasticity*, 27(2011), 1072-1092. <https://doi.org/10.1016/j.ijplas.2010.11.004>.
- [7] T. Hama, H. Takuda, Crystal plasticity finite-element simulation of deformation behavior in a magnesium alloy sheet considering detwinning, *Steel Res. Int.*, (2012), Special Edition 2012, 1115-1118.

-
- [8] T. Hama, H. Takuda, Crystal plasticity finite-element simulation of work-hardening behavior in a magnesium alloy sheet under biaxial tension, *Comput. Mater. Sci.*, 51 (2012), 156-164. <https://doi.org/10.1016/j.commatsci.2011.07.026>.
- [9] T. Hama, N. Kitamura, H. Takuda, Effect of twinning and detwinning on inelastic behavior during unloading in a magnesium alloy sheet, *Mater. Sci. Eng. A*, 583 (2013), 232-241. <https://doi.org/10.1016/j.msea.2013.06.070>.
- [10] T. Hama, Y. Tanaka, M. Uratani, H. Takuda, Deformation behavior upon two-step loading in a magnesium alloy sheet, *Int. J. Plasticity*, 82(2016), 283-304. <https://doi.org/10.1016/j.ijplas.2016.03.009>.
- [11] T. Hama, A. Kobuki, H. Takuda, Crystal-plasticity finite-element analysis of anisotropic deformation behavior in commercially pure titanium Grade 1 sheet, *Int. J. Plasticity*, 91 (2017), 77-108. <https://doi.org/10.1016/j.ijplas.2016.12.005>.
- [12] T. Hama, K. Hirano, R. Matsuura, Cylindrical cup drawing of a commercially pure titanium sheet: experiment and crystal plasticity finite-element simulation, *Int. J. Mater. Form.*, 15 (2022), 8, 23 pages. <https://doi.org/10.1007/s12289-022-01655-x>.
- [13] T. Hama, T. Suzuki, S. Hatakeyama, H. Fujimoto, H. Takuda, Role of twinning on the stress and strain behaviors during reverse loading in rolled magnesium alloy sheets, *Mater. Sci. Eng. A*, 725(2018), 8-18. <https://doi.org/10.1016/j.ijplas.2018.02.009>.